

We are IntechOpen, the world's leading publisher of Open Access books Built by scientists, for scientists

6,900

Open access books available

186,000

International authors and editors

200M

Downloads

Our authors are among the

154

Countries delivered to

TOP 1%

most cited scientists

12.2%

Contributors from top 500 universities



WEB OF SCIENCE™

Selection of our books indexed in the Book Citation Index
in Web of Science™ Core Collection (BKCI)

Interested in publishing with us?
Contact book.department@intechopen.com

Numbers displayed above are based on latest data collected.
For more information visit www.intechopen.com



Afterburning Installation Integration into a Cogeneration Power Plant with Gas Turbine by Numerical and Experimental Analysis

Ene Barbu et al*

*National Research and Development Institute for Gas Turbines COMOTI,
Romania*

1. Introduction

Gas turbines applications represent a continuous challenge for engineers regarding the design, manufacturing and efficient working at nominal and partial loads with respect to environmental and future development requirements. The development of gas turbines in terms of performances as well as of lifetime and safe running has made these installations preferable for cogenerative processes and the lower maintenance costs have lead to particularly tempting recovery terms, down to 3-4 years for a 15-20 years lifetime. The increase in the overall efficiency of the cogenerative group is affected by the degree of use of the heat produced by the gas turbine along with the flue gases. The recovery of the flue gases heat is achieved by using a heat recovery steam generator, usually for producing steam (or hot water). The performances of a heat recovery steam generator depend on the gas turbine's working regime which makes the steam parameters difficult to control. The trend in the field of heat recovery steam generator and afterburning installations are related to the development in gas turbines. The increase in the temperatures of the gas turbine requires new materials that withstand operating regimes in terms of appropriate pollutants norms. The oxygen concentration in the gas turbine's flue gases is usually of 11 - 16 % volume. The fact that the combustion process in the gas turbine consumes only a small part of the oxygen from the intake air flow makes possible the application of a supplementary firing (afterburning) for increasing the steam flow rate of the heat recovery steam generator. In aviation the afterburning is used for increasing the thrust of supersonic aircrafts equipped with gas turbines. Introducing the afterburning in cogenerative applications leads to increasing the flexibility and the overall efficiency of the cogenerative group. The burner of the afterburning installation is usually placed between the gas turbine and the heat recovery steam generator, immersed in the flue gases exhausted by the gas turbine, resulting in a complex gas turbine - afterburning - heat recovery steam generator system. This placement results in the afterburning installation affected by the gas turbine and affects the working of the heat recovery steam generator. Usually, when the heat recovery steam generator is used for delivering superheated steam, the working conditions of the afterburning installation

* Valeriu Vilag, Jeni Popescu, Silviu Ionescu, Adina Ionescu, Romulus Petcu, Cleopatra Cuciumita, Mihaiella Cretu, Constantin Vilcu and Tudor Prisecaru
National Research and Development Institute for Gas Turbines Comoti, Romania

influence mainly the superheater of the heat recovery steam generator (with effects on temperature, flow rate etc.). The design of the gas turbine – afterburning installation – heat recovery steam generator system must take into account these variables for insuring the steam parameters required by the technological process. The active control of the combustion is a concept already accepted and the new generation of afterburning installations will need to answer to the requirements of the new “smart” aggregates which automatically take into account the emissions, the energetic efficiency and the process requirements (PIER, 2002). For that purpose the researches conducted at Suplacu de Barcău 2xST 18 Cogenerative Power Plant has focused on the afterburning installation as integral part of the cogenerative group in terms of stack emissions, superficial temperature profile and power quality (Barbu et al., 2010) as well as on its interaction with the heat recovery steam generator.

2. General principles of the mathematical modelling of the thermo-gas-dynamic and chemical processes in the combustion chambers

The classical approach of the combustion chambers study assumes as a general rule the embracing of a steady character of the phenomena taking place in these installations, constituting only a quasi-adequate manner to the problem of analysing the unsteady phenomena generating important collateral effects. The physical-chemical phenomena succeeding in the combustion chamber are extremely complex, each of them (injection, atomization, vaporization, diffusion, combustion) rigorously depending on the physical factors such as air excess, gases pressure, temperature and velocity in the chamber. It may be admitted that the combustion is normal as long as the fluctuations detected in the combustion chamber only depend on the local conditions and they are randomly distributed in the chamber. The high level of complexity of the phenomena, associated to the flow instabilities, the heat transfer and the combustion reactions, makes them inaccurate to model using simplified mathematical models which only globally consider the processes and which are only slightly dependent on the combustion chamber geometry, the combustion configuration, the walls' screening or the intermediary reactions in the flame. Therefore, here is studied the complex and coupled problem of mathematical modelling for pulsating flow (numerical integration of Navier-Stokes equations with a closing model application), the influence on heat transfer (considering the radiation and convection), the combustion reactions (applying complex combustion mechanisms with high number of reactions and intermediary chemical compounds). The generalized model accurately tracking the complex processes in the combustion chamber may be developed as a group of modules, each associated to a phenomenon (flow, heat transfer, combustion reactions and dispersion phase evolution). This modular approach method allows the separate development of several sub-models with higher accuracy for a certain class of problems. Hence the problem of „closing“ the equations system describing the studied phenomenon may and has been solved by using several turbulence models: $k-\epsilon$ (standard, realisable or RNG), Reynolds-stress model, LES - large eddy simulation (high scale modelling), or lately, due to the increase in calculation efforts, DNS - direct numerical simulation.

2.1 Mathematical models used for simulating flow, heat transfer and combustion in combustion chambers

There are two fundamentally different manners used for describing the fluid flow equations: the Lagrangian and Eulerian formulations. From the Lagrangian formulation perspective

the flow field represents the movement of small, adjacent fluid elements interacting through pressure and viscous forces. The movement of each fluid element is made according to Newton's second law. This method is however impractical because of the high number of mass elements necessary for reaching a reasonable accuracy in describing the flow in a continuous environment. On the other hand the Lagrangian method deserves to be taken into consideration for biphasic flows (gas-droplet type) in describing the dispersion phase because the particles naturally constitute individual mass elements. The complexity of the Eulerian formulation of the biphasic flow does not allow the direct application of the solving schemes existing in the case of monophasic flow. As a consequence of this averaging problem in most numerical models the Lagrangian formulation is used for describing the dispersion phase. The relation between the Lagrangian and the Eulerian formulations is given by the Reynolds transport theorem. Therefore the components on the three axes may be combined in a single vectorial equation:

$$\rho \frac{D\mathbf{u}}{Dt} = \rho \mathbf{F} - \text{grad } p + \mu \nabla^2 \mathbf{u} + \frac{1}{3} \mu \cdot \text{grad}(\text{div} \mathbf{u}) \quad (1)$$

Equation (1) represents the Navier-Stokes in complete vectorial form describing the movement of a viscous fluid. The Navier-Stokes equation is applied for laminar flows as well as for turbulent flows. However it cannot be directly used in solving the problems associated to turbulent flow because it is impossible to track the minor fluctuations of the velocity associated with the turbulence. In order to determine the flow field, the numerical model solves the mass and impulse conservation equations. For flows involving heat transfer of compressibility additional equations are needed for energy conservation. For flows implying chemical compounds mixing or chemical reactions an equation of chemical compounds conservation is solved or, in the „probability density function“ cases (generically called PDF models), conservation equations for the considered mixture fractions as well as equations defining their variations are needed. In flows with turbulent character additional transport equations need to be solved. Mass conservation equation, or continuity equation, may be written:

$$\frac{\partial \rho}{\partial t} + \frac{\partial}{\partial x_i}(\rho u_i) = S_m \quad (2)$$

Equation (2) is the generalized formulation of mass conservation equation and is applicable for incompressible or compressible flows. The source term S_m represents the mass added to the continuous phase, mass resulted from the dispersion phase (due to liquid droplets' vaporization) or a different source. For axi-symmetric bi-dimensional flows, the continuity equation is given by:

$$\frac{\partial \rho}{\partial t} + \frac{\partial}{\partial x}(\rho u) + \frac{\partial}{\partial r}(\rho v) + \frac{\rho v}{r} = S_m \quad (3)$$

where x is the axial coordinate, r is the radial coordinate, u is the axial velocity and v is the radial velocity. The impulse conservation on i in an inertial reference plane is described by:

$$\frac{\partial}{\partial t}(\rho u_i) + \frac{\partial}{\partial x_j}(\rho u_i u_j) = -\frac{\partial p}{\partial x_i} + \frac{\partial \tau_{ij}}{\partial x_j} + \rho g_i + F_i \quad (4)$$

where p is the static pressure, τ_{ij} is the tension tensor and ρg_i and F_i are the internal and external gravitational forces (e.g. occurring from the interaction with the dispersion phase) on direction i . F_i also includes other source terms depending on the model (such as for porous environment case). The tension tensor τ_{ij} is given by:

$$\tau_{ij} = \left[\mu \left(\frac{\partial u_i}{\partial x_j} + \frac{\partial u_j}{\partial x_i} \right) - \frac{2}{3} \mu \frac{\partial u_l}{\partial x_l} \delta_{ij} \right] \quad (5)$$

where μ is the dynamic viscosity and the second term in the right side of the relation represents the effect of volume dilatation. For axi-symmetric bi-dimensional geometries the axial and radial impulse conservation equations are given by:

$$\begin{aligned} \frac{\partial}{\partial t}(\rho u) + \frac{1}{r} \frac{\partial}{\partial x}(r \rho u u) + \frac{1}{r} \frac{\partial}{\partial x}(r \rho v u) = -\frac{\partial p}{\partial x} + \\ + \frac{1}{r} \frac{\partial}{\partial x} \left[r \mu \left(2 \frac{\partial u}{\partial x} - \frac{2}{3} (\nabla \cdot \vec{v}) \right) \right] + \frac{1}{r} \frac{\partial}{\partial r} \left[r \mu \left(\frac{\partial u}{\partial r} + \frac{\partial v}{\partial x} \right) \right] + F_x \end{aligned} \quad (6)$$

$$\begin{aligned} \frac{\partial}{\partial t}(\rho v) + \frac{1}{r} \frac{\partial}{\partial x}(r \rho u v) + \frac{1}{r} \frac{\partial}{\partial x}(r \rho v v) = -\frac{\partial p}{\partial r} + \frac{1}{r} \frac{\partial}{\partial x} \left[r \mu \left(\frac{\partial v}{\partial x} + \frac{\partial u}{\partial r} \right) \right] + \\ + \frac{1}{r} \frac{\partial}{\partial r} \left[r \mu \left(2 \frac{\partial v}{\partial r} - \frac{2}{3} (\nabla \cdot \vec{v}) \right) \right] - 2 \mu \frac{v}{r^2} + \frac{2}{3} \frac{\mu}{r} (\nabla \cdot \vec{v}) + \rho \frac{w^2}{r} + F_r \end{aligned} \quad (7)$$

where $\nabla \vec{v} = \frac{\partial u}{\partial x} + \frac{\partial v}{\partial r} + \frac{v}{r}$ and w is the tangential velocity. The energy conservation equation may be written:

$$\frac{\partial}{\partial t}(\rho E) + \frac{\partial}{\partial x_i} [u_i (\rho E + p)] = \frac{\partial}{\partial x_i} \left(k_{ef} \frac{\partial T}{\partial x_i} - \sum_{j'} h_{j'} J_{j'} + u_j (\tau_{ij})_{ef} \right) + S_h \quad (8)$$

where k_{ef} is the effective conductivity ($k_{ef} = k + k_t$, where k_t is turbulent thermal conductivity, defined relative to the utilized turbulence model) and $J_{j'}$ is the diffusive flow of the chemical compound j' . The first three members in the left side of equation (8) represent the energy transfer due to conduction, chemical compounds diffusion and respectively viscous dissipation. The term S_h includes the heat exchanged in the chemical reactions or other volume heat sources. In equation (8),

$$E = h - \frac{p}{\rho} + \frac{u_i^2}{2} \quad (9)$$

where the sensible enthalpy h is defined, for ideal gases, by:

$$h = \sum_j m_j h_{j'} \quad (10)$$

and for incompressible flows by:

$$h = \sum_j m_j h_j + \frac{p}{\rho} \quad (11)$$

In equations (10) and (11) m_j is the mass fraction of the chemical compound j' and

$$h_j = \int_{T_{ref}}^T c_{p,j'} \cdot dT \quad (12)$$

is the corresponding enthalpy of the compound, and the reference temperature is $T_{ref} = 298.15$ K. In combustion studies, when the PDF based nonadiabatic model is used, the model requires solving an equation for total enthalpy, set by the energy equation:

$$\frac{\partial}{\partial t}(\rho H) + \frac{\partial}{\partial x_i}[\rho u_i H] = \frac{\partial}{\partial x_i} \left(\frac{k_t}{c_p} \frac{\partial H}{\partial x_i} \right) + \tau_{ik} \frac{\partial u_i}{\partial x_k} + S_h \quad (13)$$

In the hypothesis of a unitary Lewis number ($Le = 1$), the conduction and diffusion terms of the chemical compounds are combined in the first term in the left side of equation (13), while the viscous dissipation contribution in the nonconservative formulation occurs as the second term of the equation. Total enthalpy H is defined by:

$$H = \sum_j m_j H_j \quad (14)$$

where m_j is the mass fraction of the chemical compound j' and

$$H_j = \int_{T_{ref}}^T c_{p,j'} \cdot dT + h_j^0(T_{ref,j'}) \quad (15)$$

$h_j^0(T_{ref,j'})$ is the enthalpy of formation of chemical compound j' at the reference temperature T_{ref} . Equation (8) includes the terms of pressure and kinetic energy work, terms neglected in incompressible flows. The decoupled solving method for the flow equations does not require including these terms in incompressible flows. However these terms must always be considered when using coupled solving method or for compressible flows. Equations (8) and (13) include the viscous dissipation terms representing the thermal energy created by the viscous tension in the flow. When using the decoupled solving method, the energy equation formulation does not need to explicitly include these terms because the viscous heating is in most cases neglected. The viscous heating becomes important when the Brinkman number, B_r , is close or higher than the unitary value, where

$$B_r = \frac{\mu U_e^2}{k \Delta T} \quad (16)$$

and ΔT represents the temperature difference in the system. The compressible flows usually have a Brinkman number $B_r \geq 1$. In the same time equations (8) and (13) include the enthalpy transport effect due to chemical compounds diffusion. For the decoupling solving method the term $\frac{\partial}{\partial x_i} \sum_j h_j J_j$ is included in equation (8), and in the nonadiabatic combustion

model (PDF) this term does not explicitly appear in the energy equation, being included in the first term in the right side of equation (13). The energy sources S_h include in equation (8) the energy due to chemical reactions.

$$S_{h, reaction} = \sum_{j'} \left[\frac{h_{j'}^0}{M_{j'}} + \int_{T_{ref, j'}}^{T_{ref}} c_{p, j'} \cdot dT \right] \cdot R_{j'} \quad (17)$$

where $h_{j'}^0$ is the enthalpy of formation of compound j' , and $R_{j'}$ is the volumetric velocity of creation of compound j' . When using the PDF combustion model, the heat of formation is included in the enthalpy definition so the energy sources of the chemical reaction are no longer included in the formulation of S_h .

3. Suplacu de Barcau 2xST 18 cogenerative power plant

Suplacu de Barcau 2xST 18 Cogenerative Plant (fig. 1), with beneficiary SC OMV PETROM SA, is located in Bihor County, Romania, 75 km from Oradea Municipality. The main technical data are given in table 1. The plant was integrally commissioned in 2004 working in the framework of Suplacu de Barcau Oil Field. The electrical energy is used for driving the reducing gear boxes from the oil wells, the compressors, the pumps, for lighting etc. and the thermal energy (steam) is injected in the deposit being necessary in the oil extraction technological process and/or for other field requirements (heating the buildings or technological pipes). Suplacu de Barcau 2xST 18 Cogenerative Plant comprises two groups (fig. 1, right) which may work together or separately. Each group includes a ST 18 gas turbine (fig. 2, left), an afterburning installation (fig. 2, centre), a heat recovery steam generator (fig. 2, right) and additional installations. The heat recovery steam generator of each cogenerative group is a fire tube type boiler with two flue gas lines – one horizontal and the other vertical, comprising: the uncooled afterburning chamber; the superheater insuring the 300 °C steam temperature; the pressure body producing the saturated steam; the feed water heater assembly – water pre-heater insuring the necessary parameters of the water supplying the pressure body. The superheater is a coil type heat exchanger with 12 coil pipes (ø 38) welded in the steam inlet down-tanks (upper tank – fig. 3, centre) of the pressure body and superheated steam outlet (lower tank – fig. 2, right). The steam in the pressure body enters the upper tank through a PN40 DN150 connector (placed in the middle of the tank) and is distributed to the 12 coil pipes, then enters the lower tank and is delivered to the users.

The gases from the afterburning chamber follow the horizontal line of the heat recovery steam generator (superheater – pressure body) then the vertical one (feed water heater – water pre-heater – stack). Each cogenerative group is able to work in any of the three versions given in table 1, but the basic one is version I. 2xST 18 Cogenerative Power Plant is working automatically, the exploitation personnel being alerted by the command panel, through optical signalling and alarm horns, regarding the deviations of the supervised parameters or the damages occurrence. Certain parameters (pressures, temperatures, flow rates etc) of the equipments are archived and displayed with the help of an acquisition system.



Fig. 1. 2xST 18 Cogenerative Power Plant view (left) and gear placement (right)

No	Name	Version I	Version II	Version III
1	Cogenerative group version	Gas turbine + afterburning + heat recovery steam generator	Gas turbine + heat recovery steam generator	Heat recovery steam generator + afterburning
2	Fuel	Natural gas		
3	Gas turbine type	ST 18 (Pratt & Whitney - Canada)		
4	Boiler type	Fire tube boiler (SC UTON SA Onesti - Romania)		
5	Electric generator type	GSI-F (Electroputere Craiova - Romania)		
6	Electrical power delivered by the plant	2x1,75 MW (6,3 kV, 50 Hz)		-
7	Superheated steam pressure	20 bar		
8	Superheated steam temperature	300 °C		

Table 1. Technical specifications of 2xST 18 Cogenerative Power Plant



Fig. 2. ST 18 gas turbine (left), afterburning installation burner (centre) and heat recovery steam generator (right) at 2xST 18 Cogenerative Power Plant



Fig. 3. Superheater of the heat recovery steam generator at 2xST 18 Cogenerative Power Plant

3.1 The afterburning installation at Suplacu de Barcau 2xST 18 cogenerative power plant

The afterburning installation (burner with automatics) at 2xST 18 Cogenerative Power Plant was delivered by Saacke (www.saacke.com – Germany) and has the specifications given in table 2. The burner (fig. 4), produced by Eclipse – Holland, is the “FlueFire” type dedicated to this kind of application. It may be placed directly in the flue gases flow, between the turbine and the recovery boiler, but may work as well on fresh air. The burner has 21 basic modules located on 3 natural gas fuelling ramps and 2 flame propagation modules. The flue gases from the gas turbine are introduced in the “FlueFire” burner through an adaptation section. The mixture with the fuel is obtained through the swirling motion of the flue gases exhausted from the turbine in the fuel jets. This leads to the cooling and the stabilization of the combustion in the burner front allowing downstream high temperatures at a low NO_x content. The air, delivered by a fan (fig. 4, right), is introduced in the adaptation section through a distribution system built to insure an uniform distribution in the transversal section because the emissions depend on the unevenness of the flow, velocity, oxygen concentration etc. The afterburner modules are built in refractory steel, laser cut, for insuring the necessary uniformity. Each module is fitted in the natural gas fuelling ramps using two gas nozzles in order to allow the free dilatation of the assembly. The ignition is initiated with the help of a pilot burner placed in the lower area of the afterburning burner and the supervision of the flame is insured by a UV type “DURAG D-LX 100 UL” detector placed in the upper area.

No.	Name		Value
1	Natural gas pressure	Before the regulator	0,5-2 bar
		After the regulator	0,4 bar
2	Thermal power	With flue gases (version I)	2,4 MW
		With air at 20 °C (version III)	6 MW
3	Flue gases maximum mass flow rate		8,75 kg/s
4	Flue gases temperature at the inlet of the burner		524 °C
5	Flue gases temperature at the end of the afterburning chamber (versions I and III)		770 °C

Table 2. Technical specifications regarding the afterburning installation at 2xST 18 Cogenerative Power Plant

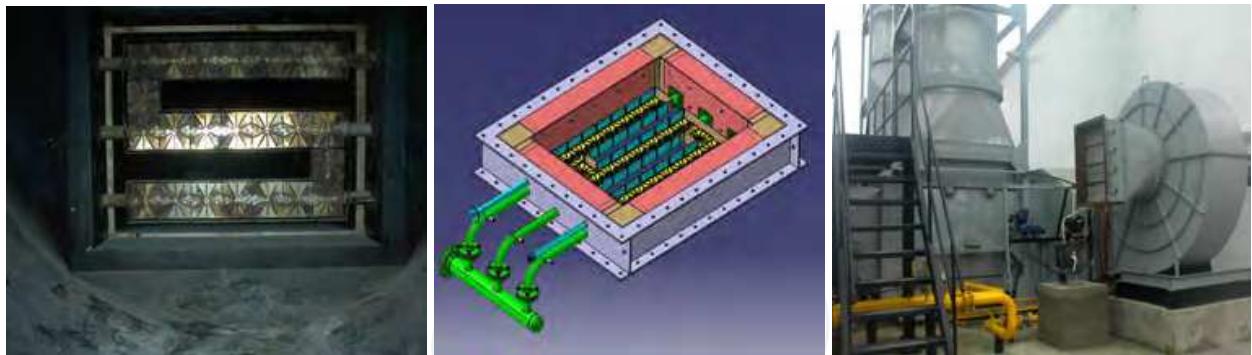


Fig. 4. The burner in the afterburning installation at 2xST 18 Cogenerative Power Plant (left, centre) and the fresh air fan (right)

4. Gas turbine – afterburning interaction

The flue gases flow in the outlet section of the gas turbine is generally turbulent and unevenly distributed. In some areas at the inlet of the afterburning installation backflows may occur. A uniform flow distribution is an important factor concurring to the good working of the afterburning and to the performances of the heat recovery steam generator. Grid type burners are designed to distribute the heat uniformly in the transversal section of the heat recovery steam generator, fact requiring careful oxygen feeding in order to avoid high NO_x emissions and variable length flame. The flow rate, the temperature, the composition of the flue gases exhausted from the gas turbine depend on the fuel type, load, fluid injection in the gas turbine (water, steam), environmental conditions etc. The gas turbines used in industrial applications are fuelled by liquid or gaseous fuels. Regarding the liquid fuels, for economical reasons, there are usually used cheap fuels such as heavy fuels, oil fuels or residual products from different manufacturing processes or chemisation (Carlanescu et al., 1997). Using these types of fuels raises problems concerning: insuring combustion without coating, decreasing the corrosive action caused by the presence of aggressive compounds (sulphur, traces of calcium, lead, potassium, sodium, vanadium) and problems concerning pumping and spraying (heating, filtration etc.). When considering using aviation gas turbines for industrial purposes (existing aviation gas turbines with minimal modifications) the possibilities of using liquid fuels are limited. For each case the technical request of the beneficiary must be analyzed in conjunction with the study of fuel characteristics affecting the processes in the combustion chamber (density, molecular mass, damping limits, burning point, volatility, viscosity, superficial tension, latent heat of vaporization, thermal conductivity, soot creation tendency etc.). For the gaseous fuels the problem is easier considering the high thermal stability, the absence of soot and ashes, and the high caloric power. In this case the problems concern mostly the combustion process in conjunction with the requirements of the used gas turbine. For the valorisation of the landfill gas the TV2 – 117A gas turbine was modified to work on landfill gas instead of kerosene by redesigning the combustion chamber (Petcu, 2010). Numerical simulations and experimentations have been conducted for the gas turbine working on liquid fuel (kerosene) and gaseous fuels (natural gas, landfill gas). The boundary conditions have been either calculated or delivered by the gas turbine manufacturer for three working regimes: take-off, nominal and idle. The results are presented in table 3 with the corresponding temperatures for each regime. The temperature fields are displayed in rainbow with red representing the

highest value. The most important result refers to the fact that the numerically obtained temperatures are close enough to the ones indicated by the manufacturer, the differences being explained by the simplifying hypotheses introduced in the simulations. Analyzing the numerical results it may be observed that the flame shortens (column 5) with the decrease in regime, but it fills better the area between two adjacent injectors (column 6). The main criterion validating the numerical results has been the averaged turbine inlet temperature (T_m) in the conditions of fuel and air flow rate imposed by the working regimes of the TV2 – 117A gas turbine. For working on gaseous fuel, the TV2 – 117A gas turbine has suffered adjustments on the fuel system level and particularly on the injection nozzles. The starting point in designing the new injection nozzle was a previous application on the TA2 gas turbine resulted by modifying the TV2 – 117A. Table 4 presents the variation of the CH_4 mass fraction indicating the injected jet shape (left) and the burned gases temperature in the combustion chamber outlet/turbine inlet section (right) for different working regimes. The geometrical parameters of the injection nozzle were set based on the numerical temperature fields in the turbine inlet section and aiming to obtain a compact fuel jet which avoids the combustion chamber walls. It must be noted that a stable combustion process has been obtained using a gaseous fuel in a combustion chamber designed for a different type of fuel (kerosene). The numerical simulations made possible narrowing the variation domains for the geometrical and gas-dynamic parameters in order to establish the constructive solution of the combustion chamber for working on landfill gas. The numerical results have been used for designing and manufacturing the new injection nozzle for the eight injectors of the TV2 – 117A gas turbine, transforming it into the TA2 aero-derivative. From tables 3 and 4 it may be noticed that by changing the fuel and the working regime the temperature distribution in the section of interest is modified, fact that might affect the afterburning installation performances. For reducing the NO_x emissions, reducing the temperature in the combustion area is applied through water or steam injection.

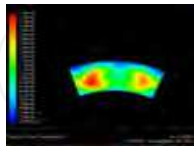
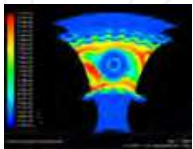
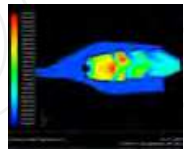
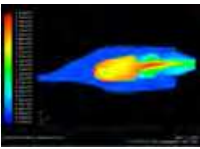
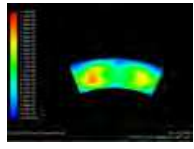
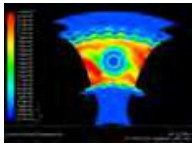
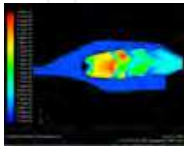
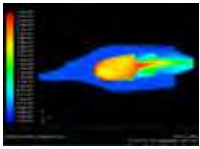
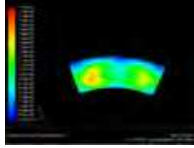
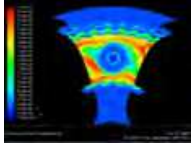
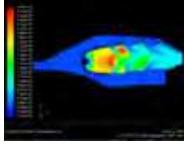
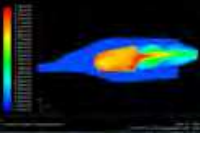
Regime	T_m [K]	Thermal field at the outlet	Thermal field on the walls	Thermal field in the axial- median section	Thermal field on the frontier between two sections
1	2	3	4	5	6
Take-off	1135				
Nominal	1075				
Cruise	1039				

Table 3. Numerical results for the TV2 – 117A gas turbine on liquid fuel (Petcu, 2010)

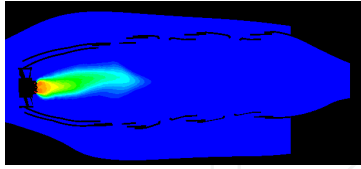
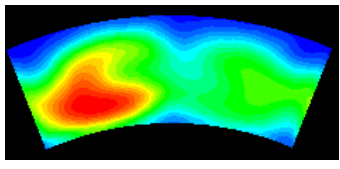
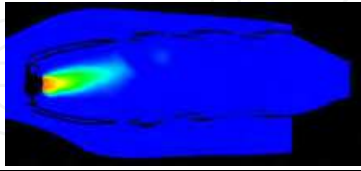
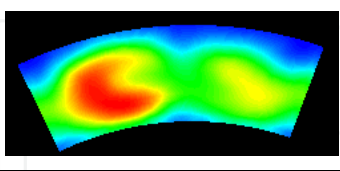
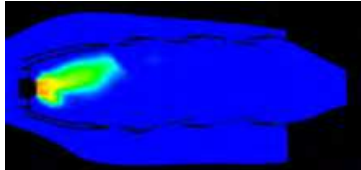
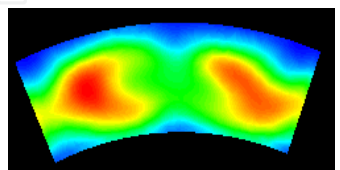
No.	T _m [K]	Fuel injection jet	Combustion chamber outlet temperature field
1	1053		
2	952		
3	944		

Table 4. Numerical results for the TA2 gas turbine on landfill gas - injection jet and thermal cross section from numerical simulations (Petcu, 2010)

In some cases the water or steam are injected directly in the combustion area through a number of holes in the combustion chamber inlet section or in the fuel injection nozzle. Another solution is injecting the water upstream of the firing tube, usually in the air flow that next passes the turbulence nozzles in its way to the combustion area. This method insures a very good atomization, the small droplets being transported by the air flow while the larger ones form a thin film on the surface of the turbulence nozzles being next atomized by the air passing over the downstream edges of the turbulence nozzle. The efficiency of the water or steam injection in reducing the NO_x emissions has been highlighted by many authors and may be expressed by the following relation (Carlanescu et al., 1998):

$$\frac{NO_{x(wet)}}{NO_{x(dry)}} = \exp-(0.2x^2 + 1.41x)$$

(18)

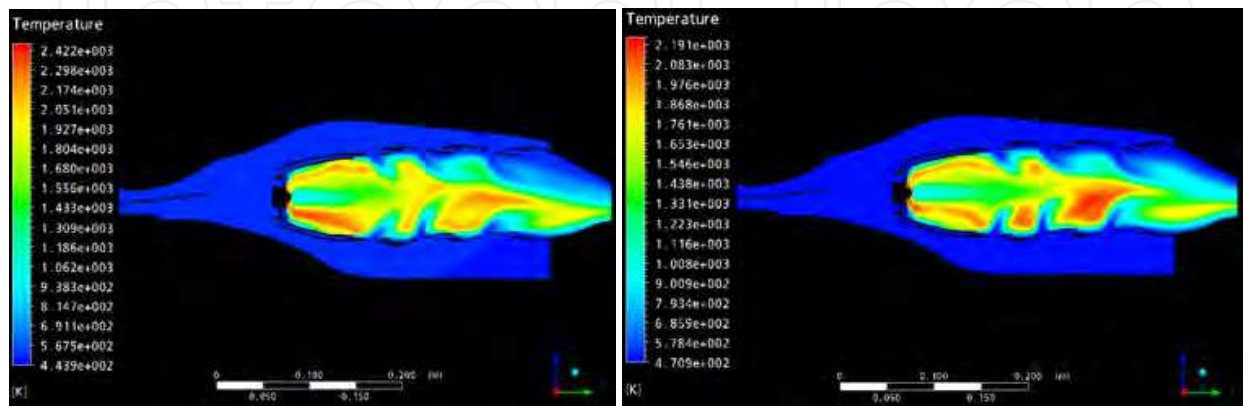


Fig. 5. Temperature field in the axial-median section of the TA2 combustion chamber, T_m =1063 K, without water injection (left) and with water injection (right) (Popescu et al., 2009)

Relation (18) may be applied for liquid as well as for gaseous fuels, showing that approximately 80 % reduction in the NO_x emissions may be obtained at equal water/steam-to-fuel flow rates ($x = 1$). The water injection is more efficient at higher combustion pressures and temperatures where the NO_x production is higher and less efficient at lower pressures and temperatures. For the independent running of the TA2 gas turbine on methane, without afterburning, the numerical simulations (fig. 5 – 6) regarding the water injection have shown a NO_x reduction of over 50 % (Popescu et al., 2009).

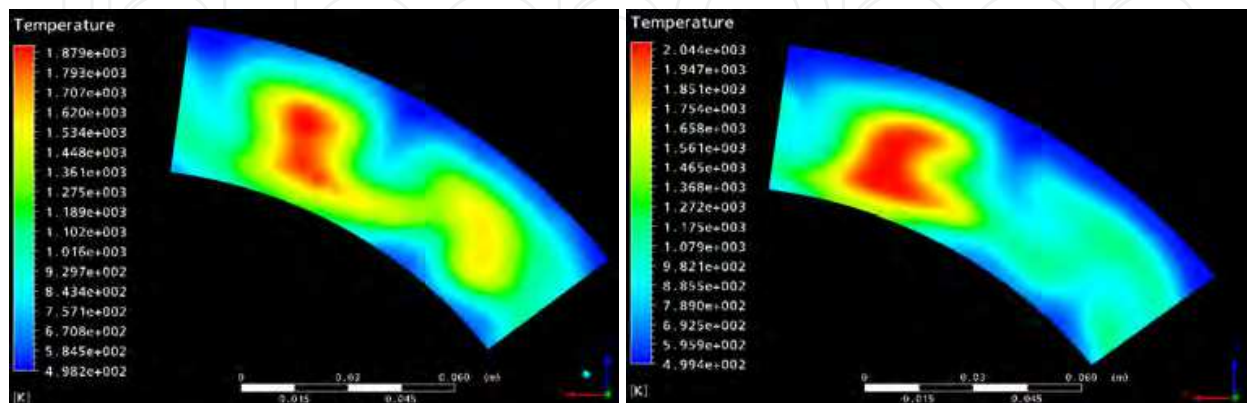


Fig. 6. Temperature field in the combustion chamber outlet section, $T_m = 1063$ K, without water injection (left) and with water injection (right) (Popescu et al., 2009)

However, theoretical and experimental researches on a turbojet have shown that the steam injection reduces the NO emissions up to 16% (mass fractions) when a steam flow which doubles the fuel flow is introduced (Benini et al., 2009). At the same ratio, the NO reduction in the water injection case is approximately 8%. The steam injection slightly reduces the CO level while the water injection raises it with the increase in the injected water quantity. Using the NASA CEA program (McBride & Gordon, 1992; Zehe et al., 2002), the combustion have been analyzed in the TA2 gas turbine for methane, natural gas (the composition at Suplacu de Barcau Cogenerative Plant) and landfill gas (equal volume proportions of methane and carbon dioxide) in the pressure and temperature conditions recommended for different working regimes of the gas turbine ($T_m = 1063, 1023$ and 873 K). The air excess coefficients have been established for each fuel in the dry working cases in order to obtain the same temperature of the reaction products for a corresponding fuel quantity. Starting from these initial data and increasing the injected water quantity up to 50 % of the fuel quantity, a decrease in temperature has been noticed for each 10 % injected water of approximately 1.46 degrees for methane, 1.62 degrees for natural gas and 1.36 degrees for landfill gas. It was then aimed to establish the dependence of the quantitative water-to-fuel ratio at supplementary fuel injection in order to maintain the maximum temperature in the gas turbine. These analysis have been made only for methane for the same stable working regimes of the TA2 gas turbine ($T_m = 1063, 1023$ and 873 K). In the theoretical calculations for methane some limitations have been next applied: a ratio between the fuel quantity in the water injection case and the initial fuel quantity of maximum 2; a minimum oxygen concentration in the flue gases from the gas turbine of 11 % volume for afterburning running. The general reaction for methane combustion when water injection is involved is given by equation (19) and the algorithm used in the NASA CEA program for determining the water injection influence is presented in fig. 7:

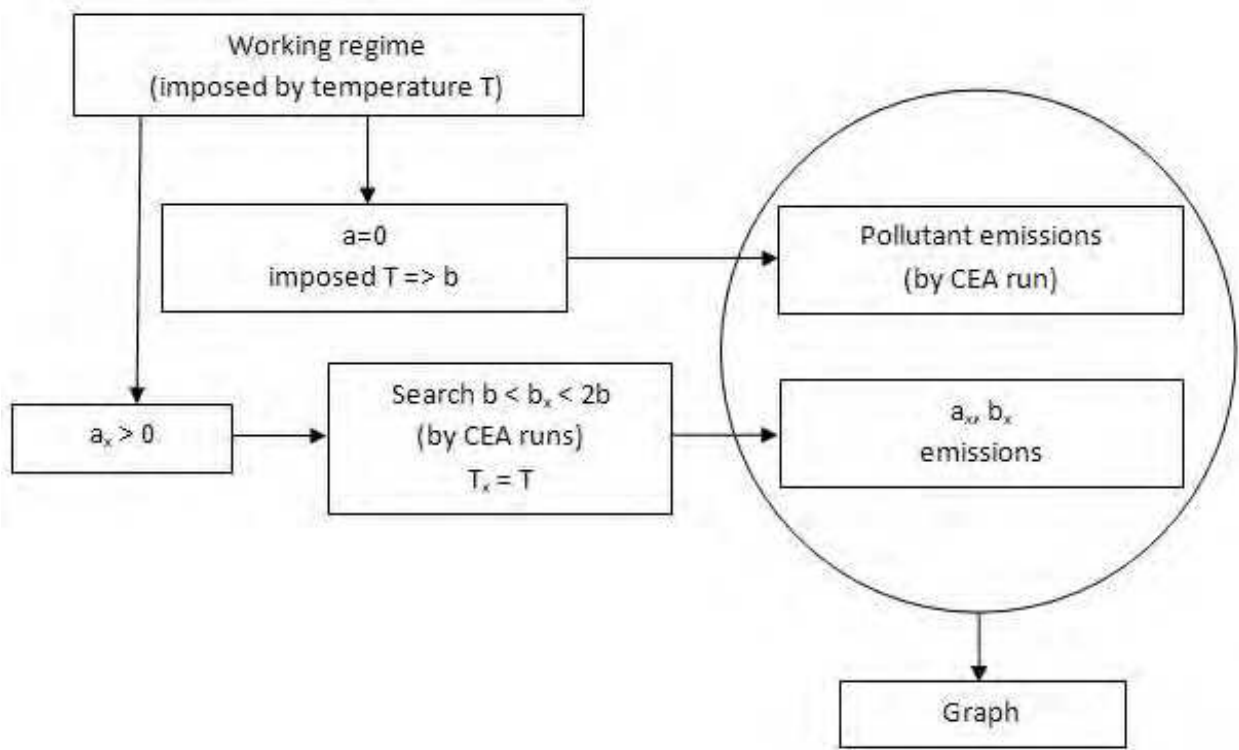
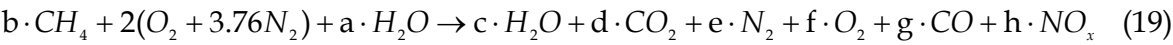


Fig. 7. The algorithm used in NASA CEA program to determine the water injection influence (subscript „x“ denominates the seeked coefficients for the desired fixed temperature)

The thermodynamic properties of the system have been tracked with focus on the reaction products concentrations and particularly CO and NO_x. In these conditions the calculations have been made for a water coefficient (denoted a) of maximum 8 (fig. 8). For a higher value than 6.5 an instability of the curves occurs. For a value of the coefficient of approximately 2.8, the gas turbine at the regime T_m = 1063 K is close to the minimum oxygen limit of 11% needed for the afterburning. In fig. 9 and 10 the water coefficient a is limited to 4. Therefore we may have a maximum water coefficient of 2.8 for the regime T_m = 1063 K, 3.1 for the regime T_m = 1023 K and 3.5 for the regime T_m = 873 K, having as result the inaccessible areas of emissions reduction for the TA2 gas turbine with water injection when using the afterburning. The theoretical calculations indicate that the NO_x emissions for the TA2 working at the regime T_m = 1063 K with afterburning may not be lower than 40 ppm. The unevenness of the flow when exiting the combustion chamber (tables 3 and 4, fig. 5 and 6) and the variation in the burned gases composition (fig. 8 – 10) affect the afterburning process and confirm the necessity of a fine control on the injected water quantity particularly when a significant reduction of the emissions is aimed. Therefore the afterburning is affected from the efficiency, emissions, flame stability points of view as well as from the corrosion on the elements subjected to the burned gases action. The combined actions of water vapours and oxygen concentration and high temperature of the flue gases represent the recipe for an accentuated corrosion (Conroy, 2003).

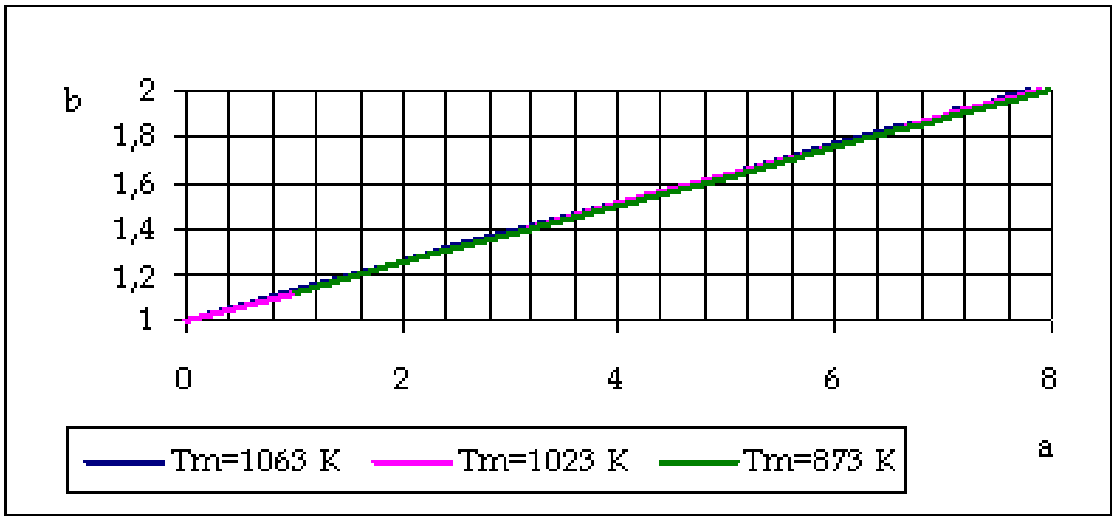


Fig. 8. Fuel coefficient (b) variation depending on injected water coefficient (a)

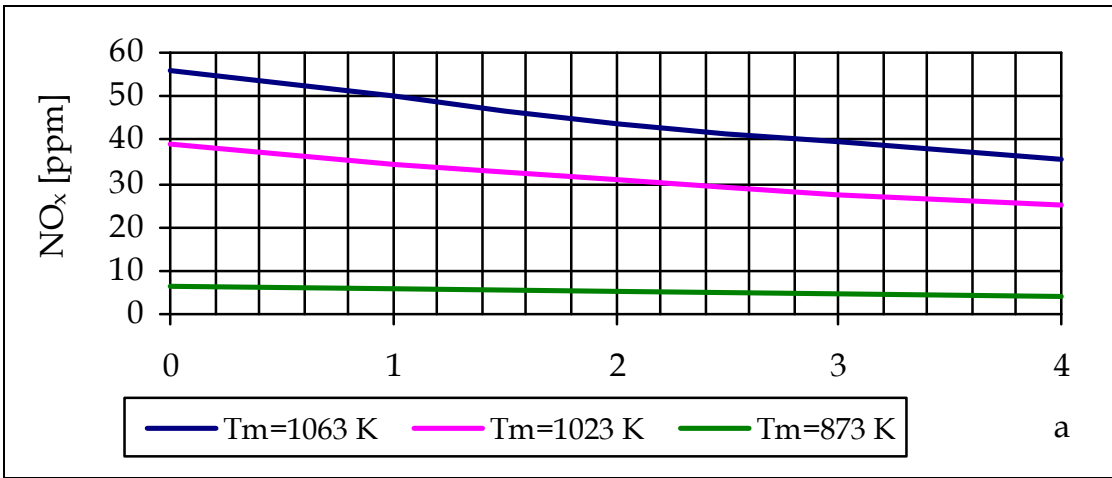


Fig. 9. NO_x concentration variation depending on injected water coefficient (a)

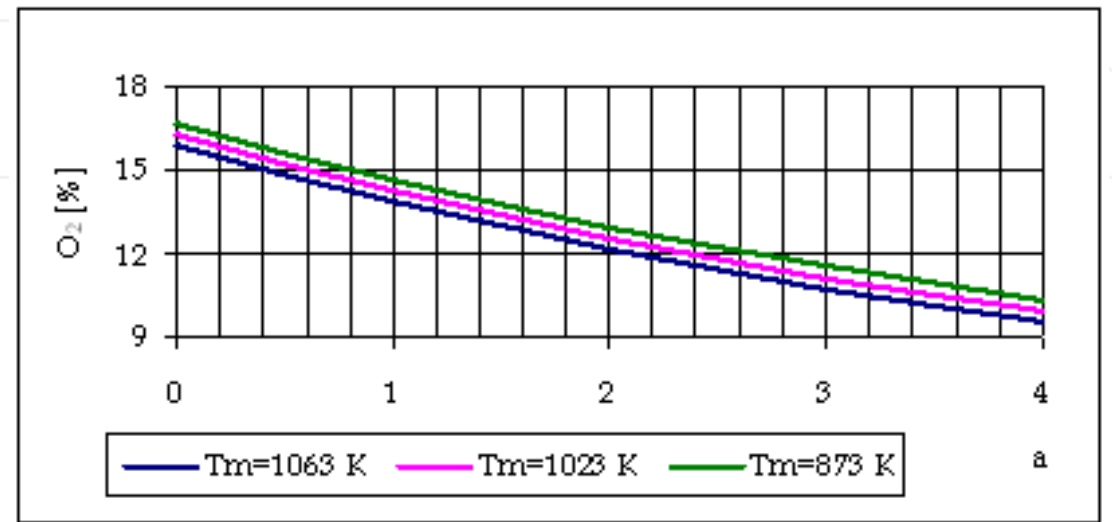


Fig. 10. O₂ concentration variation depending on injected water coefficient (a)

5. Afterburning – Heat recovery steam generator interaction

The heat recovery steam generator in the cogenerative groups is designed to run at certain parameters of the flue gases and superheated steam. The process requirements, the variable environmental conditions (affecting the gas turbine and therefore the afterburning) influence the running of the heat recovery steam generator and the overall efficiency of the cogenerative group. The steam superheater is usually the last heat exchanger in the pressurized thermal circuit water – steam of a heat recovery steam generator. As „end of the line“ element it is its duty to maintain the temperature of the superheated steam, imposing mechanical systems and automatics with well defined functions and roles taken into consideration by the designer. Increasing the nominal parameters of modern heat recovery steam generator as a result of the increased performances in gas turbines led to a superheater area larger than that of the vaporizing system, the superheater becoming a large metal consumer as well as the heat exchanger with the highest thermal demand. As consequence, the superheater needs the proper consideration in the design process as well as in activity. If the flow process in the superheater pipes is admitted as isobar, the increase in temperature takes place according to an exponential law. The value of the coefficient of thermal unevenness in the flue gases flow entering the superheater stage depends on the constructive shape and the thermal diagram. This coefficient is defined by (Neaga, 2005):

$$k'_t = \frac{t'_{g\max} + 273}{t'_{g\text{med}} + 273} \quad (20)$$

where the index shows that the temperatures are indicated for the inlet of the stage, $t'_{g\max}$ and $t'_{g\text{med}}$ being the maximum and respectively the averaged temperatures of the gases at the inlet. The ability of the steam to absorb the heat of the flue gases in different areas of the volume occupied by the stage leads to unevenness affecting the safe running of the heat exchanger. The researches show that the highest unevenness on the outlet of the stage is registered in the counter-stream flow of the thermal agents regardless of the number of stages of the superheater and the lowest in the uniflow (Neaga, 2005). The characteristics of the superheated steam are different for the radiation and convection superheaters. The radiation superheater absorbs more heat at low loads while the convection one absorbs more heat at higher loads (Ganapathy, 2001). The superheaters usually have more stages, the radiation and convection combined ensuring a uniform temperature in the steam for a larger range of loads. When the superheater consists in only one stage the problem of controlling the temperature in the superheated steam becomes more complicated. The steam temperature can usually be maintained constant in the 60 – 100 % load range but several factors act on the superheated steam temperature: heat recovery steam generator load, air excess coefficient at the furnace outlet, initial dampness of the fuel, calorific value of the fuel etc. As consequence, the temperature control systems must comply with certain conditions: low inertia, large control range (regardless of the variable parameter leading to variations in the superheated steam temperature), safe running construction, minimal manufacturing and running expenses etc.

6. Researches concerning the integration of the afterburning installation with the gas turbine and the heat recovery steam generator at Suplacu de Barcau 2xST 18 cogenerative plant

6.1 The integration of the afterburning installation with the heat recovery steam generator

The researches for the integration of the afterburning installation with the heat recovery steam generator and the gas turbine at Suplacu de Barcau 2xST 18 Cogenerative Power Plant have been made in several stages. At commissioning, the functional tests at some working regimes of the heat recovery steam generator have shown high temperatures of the superheated steam (table 5) compared to the nominal temperature (300 °C), leading to frequent activations of the heat recovery steam generator. In these conditions the coil pipes have been counted, from 1 to 12 (fig. 11), in the direction of the steam circulation through the lower tank, the outer temperature has been measured (fig. 3, 11) with a contact thermometer (Barbu et al., 2006) and the exchange area of the superheater has been reduced by replacing the first three coil pipes with three L-shaped pipes in order to maintain the steam velocity. Fig. 12 presents the temperature distribution on the outer surface of the 12 coil pipes of the superheater's outlet tank (t_{eSI}) after the replacement, for the averaged temperature of the superheated steam $t_{vSI}= 280\text{ }^{\circ}\text{C}$ and the temperature of the gases at the afterburning chamber outlet $t_{ca}=690\text{ }^{\circ}\text{C}$.

Coil pipe	2	4	6	8	10	12	Observations
Outer temperature [°C]	370	380	295	295	245	185	Before replacement; $t_{vSI}= 322\text{ }^{\circ}\text{C}$
	210	398	366	364	212	198	After replacement; $t_{vSI}= 280\text{ }^{\circ}\text{C}$

Table 5. Outer temperature of the coil pipes of the superheater’s outlet tank

The data in table 5 and fig. 12 (left) shows a modification in temperature distribution after the replacement of the three coil pipes. In the end, the pipes 1 – 4 have been cut and plugged and refractory metal sheets have been applied on each superheater (for a better circulation of the flue gases in the superheater) leading to the temperature distribution presented in fig 12 (right). Fig. 12 (right) illustrates an increase in the thermal field evenness in the coil pipes compared to the initial case at the commissioning of the heat recovery steam generator (table 5). For the process requirements of superheated steam temperature up to 350 °C only the area of the screens has been adequately reduced.

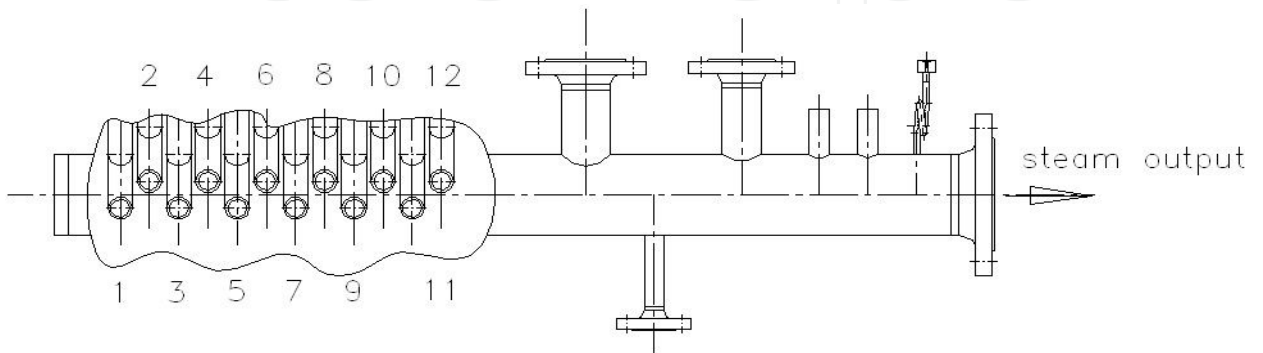


Fig. 11. Counting of the coil pipes of the superheater’s outlet tank

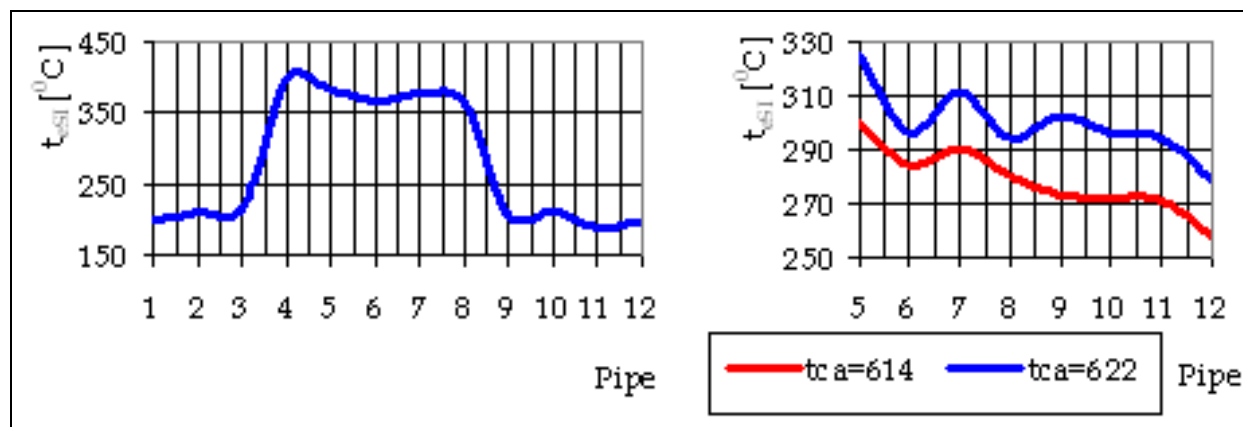


Fig. 12. Outer temperature (t_{eSI}) variation in the outlet tank after replacing the coil pipes 1 - 3 with three L-shaped pipes ($t_{vSI}=280$ °C, $t_{ca}=690$ °C - left) and after plugging the coil pipes 1 - 4 and installing the screens on the superheater ($t_{ca}=614$ °C s and 622 °C - right)

6.2 The integration of the afterburning installation with the gas turbine

The data obtained until present resulted from experimentations conducted at 2xST 18 Cogenerative Plant, numerical simulations in CFD environment and experimentations with natural gas and air on the test bench.

6.2.1 The afterburning integrated analysis system

After solving the problem of the superheated steam temperature control, the next step has been simulating in CFD environment the afterburning installation at Suplacu de Barcau 2xST 18 Cogenerative Plant (Barbu et al., 2010). The numerical results have indicated that the air (or flue gases from the gas turbine) distribution in the burner may be improved leading to the installation of a concentrator at group 1. The second cogenerative group has remained unmodified since the commissioning. For determining the influence of the concentrator on the combustion process several aspects have been analysed: emissions at the stack, noise, superficial temperature profile and power quality for different working regimes of the groups. The measurements have been performed in industrial conditions on both cogenerative groups before applying overall optimization solutions in order to not disturb the technological process. For this reason the measurements have been performed for partial loads. For noise analysis have been used three measuring chains and a software application for acoustic prediction according to 2002/49/EC Directive, offering an image of the noise propagation in the area of interest. The noise measurements at the afterburning installation have been performed with a 01dB Metravib SOLO sound level meter. The acoustic field in the station's area has been studied in 50 measuring points with the B&K 2250 sound level meter and the acoustic pressure level of the cogenerative group has been determined with the multi-channel acquisition system 01dB Metravib EX-IF10D/module IEPE with 12 microphones 40AE G.R.A.S.. The measurements concerning the quality of environmental air have been performed with the help of the mobile laboratory (fig. 13, left) especially equipped for the task. For the chemical measurements has been used a Horiba PG 250 gas analyzer with the probe installed at the stack (fig. 13, centre). The outer superficial temperature profile has been determined with the help of a Fluke infrared camera, Ti45FT type, the sighting being in the upper area of the burner (fig. 13, right).



Fig. 13. Mobile laboratory at INCDT COMOTI (left), emissions measurements at the stack (centre) and sighting area of Fluke camera (Ti45FT type) with sound level meter (right)

The process parameters of the gas turbine, heat recovery steam generator and afterburning installation have been displayed in the command room or locally. The correlation of the emissions, noise, superficial temperature profile and power quality has been made related to the time of measurements. The electro-energetic measurements have been made in the electric generator cell through measurement converters, the equipment consisting in devices fixed in panels (ammeters, voltmeters, active and reactive energy counters) and mobile devices (CA 8332B analyser for electro-energetic network and power quality).

6.2.2 Experimental data and numerical simulation of the afterburning at 2xST 18 cogenerative plant

For starters a noise map for cogenerative group 2 has been established (without air concentrator), with group 1 out of work (fig. 14), in order to acquire comparison data for the case of local recording of noise at the burner of the afterburning installation. In the burner area the noise level has been in the 80 – 85 dB range with a significant distortion of noise curves and high values in the area of turbo-generators room. The measurements on group 1 (with concentrator) regarding emissions, noise and outer superficial temperature profile have been performed for the case of the heat recovery steam generator running with the afterburning on fresh air.

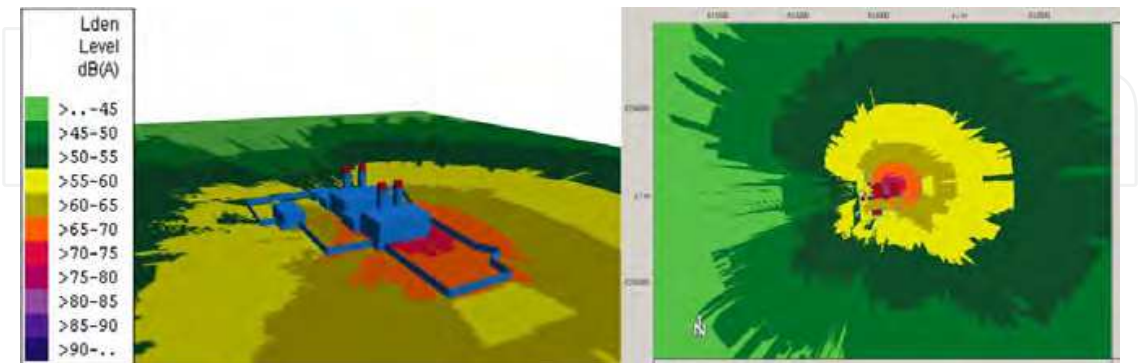


Fig. 14. Suplacu de Barcau 2xST 18 Cogenerative Plant – noise map for group 2, with group 1 out of work

Emissions, noise and outer superficial temperature profile measurements have been performed for group 1 (with concentrator) for the case of the heat recovery steam generator running with the afterburning on fresh air, with group 2 working in cogeneration (gas

turbine + afterburning + heat recovery steam generator). The set of experimental data has been obtained for five working regimes defined by the gases temperature at the outlet of the afterburning chamber (t_{ca}): 500 °C, 552 °C, 604 °C, 645 °C, 700 °C. The NO_x variation and the noise locally measured at the burner (fig. 13) for group 1 (heat recovery steam generator + afterburning on fresh air) depending on flue gases temperature are given in fig. 15. The flue gases temperature has been measured with a thermocouple at the outlet of the afterburning chamber.

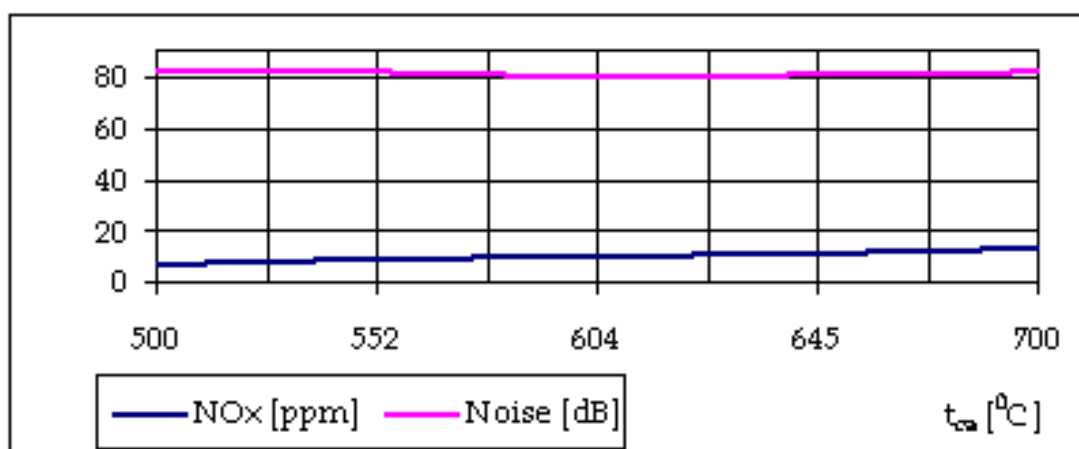


Fig. 15. NO_x and noise variation depending on flue gases temperature – group 1 (heat recovery steam generator + afterburning on fresh air)

Fig. 15 illustrates an increase in NO_x emissions with the flue gases temperature, while the noise level is approximately constant at 80 dB. For the outer superficial temperature profile, according to fig. 13 (right), an increase may be noticed in the area of the isotherms above 200 °C (fig. 16, left) with the increase in the temperature at the outlet of the afterburning chamber from 500 °C to 645 °C. The measurements on group 2 (without concentrator) regarding emissions, noise, outer superficial temperature and power quality have been performed for two cases: without afterburning (gas turbine + heat recovery steam generator) and with afterburning (gas turbine + afterburning + heat recovery steam generator). Another two sets of experimental data have been obtained. One set corresponds to three working regimes of the gas turbine + heat recovery steam generator version, defined by the flue gases temperature at the outlet of the afterburning chamber (t_{ca}): 423 °C, 437 °C, 475 °C. Another set corresponding to the version gas turbine + afterburning + heat recovery steam generator led to the following temperatures (t_{ca}): 536 °C, 569 °C, 605 °C, 645 °C. The configuration of the isotherms for the gas turbine + afterburning + heat recovery steam generator version is given in fig 16 (right). Working at fresh air rating, more than 645 °C, the region occupied by the isotherms is reduced. This area is however larger than the one for group 2 (without concentrator – fig 16, right) in gas turbine + afterburning + heat recovery steam generator version or gas turbine + heat recovery steam generator version. The central areas occupied by the isotherms (near the afterburning chamber) for group 2 (without concentrator) are decreasing with the increase in flue gases temperature at the outlet of the afterburning chamber. As opposite, for group 1, as stated above, the areas occupied by the isotherms are increasing with the increase in flue gases temperature.

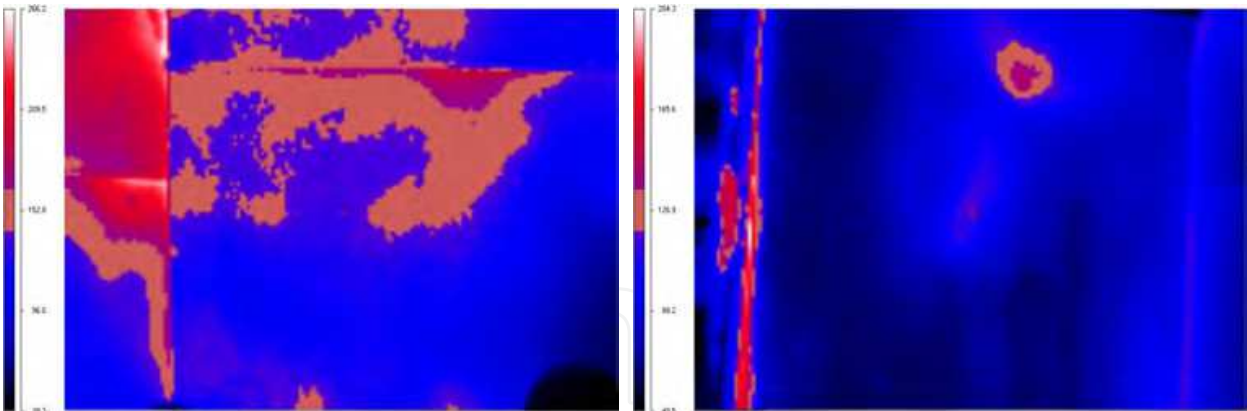


Fig. 16. Isotherms configuration for groups 1 and 2 in infrared; $t_{ca} = 645\text{ }^{\circ}\text{C}$; left – group 1 (with concentrator): heat recovery steam generator + afterburning on fresh air; right – group 2 (without concentrator): gas turbine + afterburning + heat recovery steam generator

Local noise measurements near the burner confirm the values in fig. 14. The figures 17 – 19 present the electro-energetic measurements, respectively the power variations at the generator’s hubs and the distortion coefficients from the fundamental (THD) for current and voltage depending on the flue gases temperature at the outlet of the afterburning chamber.

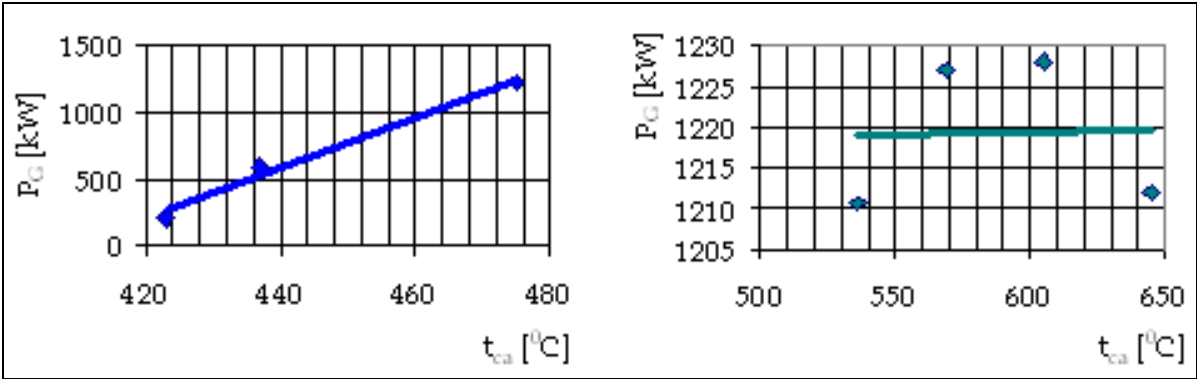


Fig. 17. Electrical power variation for version gas turbine + heat recovery steam generator (left) and version gas turbine + afterburning + heat recovery steam generator (right) depending on the flue gases temperature at the outlet of the afterburning chamber

In version gas turbine + heat recovery steam generator the variation in the heat recovery steam generator load is achieved through the variation of the gas turbine parameters. The electrical power increases with the increase in flue gases temperature (fig. 17, left). For the version gas turbine + afterburning + heat recovery steam generator the heat recovery steam generator load is varied through the afterburning parameters which makes the power quasi-constant (approximately 1220 kW) while the temperature at the outlet of the afterburning chamber increases (fig. 17, right). For the version gas turbine + heat recovery steam generator the value of the distortion coefficients from the fundamental (THD) for current and voltage decreases with the increase in temperature at the outlet of the afterburning chamber (fig. 18, 19 left).

This decrease is more pronounced for the currents (fig. 18, left) indicating an aggravation in the power quality. For version gas turbine + afterburning + heat recovery steam generator the value of the distortion coefficients from the fundamental for current and voltage

decreases only slightly (under 1%) with the increase in the flue gases temperature at the outlet of the afterburning chamber (fig. 18, 19 right).

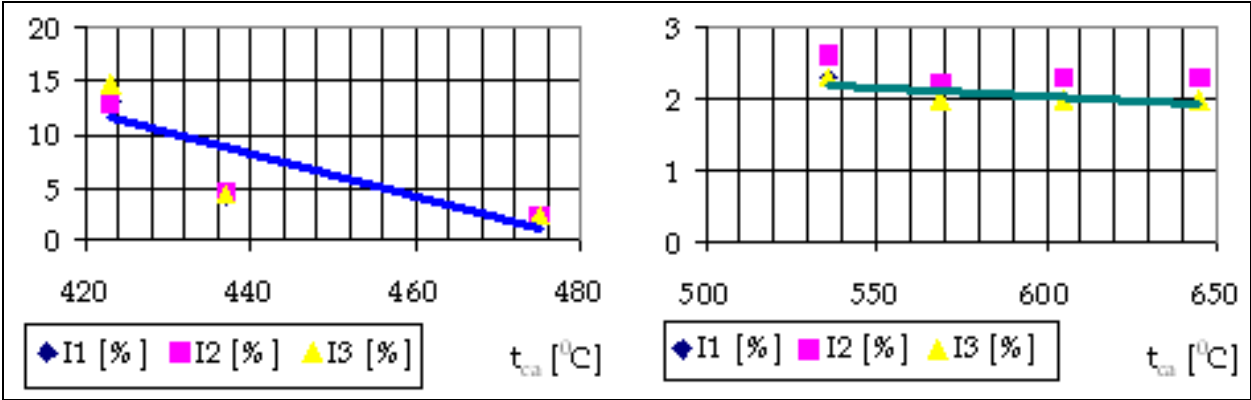


Fig. 18. Variation of distortion coefficients from the fundamental (THD) for current depending on the flue gases temperature at the outlet of the afterburning chamber for version gas turbine + heat recovery steam generator (left) and version gas turbine + afterburning + heat recovery steam generator (right)

For version gas turbine + heat recovery steam generator the variation of the distortion coefficients from the fundamental for current is higher than 5 % (fig. 18, left). This occurs at temperatures at the outlet of the afterburning chamber below 470 °C. The experiments conducted at 2xST 18 Cogenerative Plant have shown an improvement of the flow in the burner section at group 1, particularly in the upper area, but have not allowed an assessment of the performances due to geometric modification of the ST 18 burning module. Based on the experimental data obtained at Suplacu de Barcau 2xST 18 Cogenerative Plant, a new geometry has been obtained for the burning module (ST 18-R, fig. 20 left) analysed through numerical simulations in CFD environment. The new module incorporates an air (flue gases) concentrator and the module ST 18 has been angled to 15° (module ST 18-15) leading to an increased turbulence and a better mixing of the gas fuel with the comburent (Barbu et al., 2010).

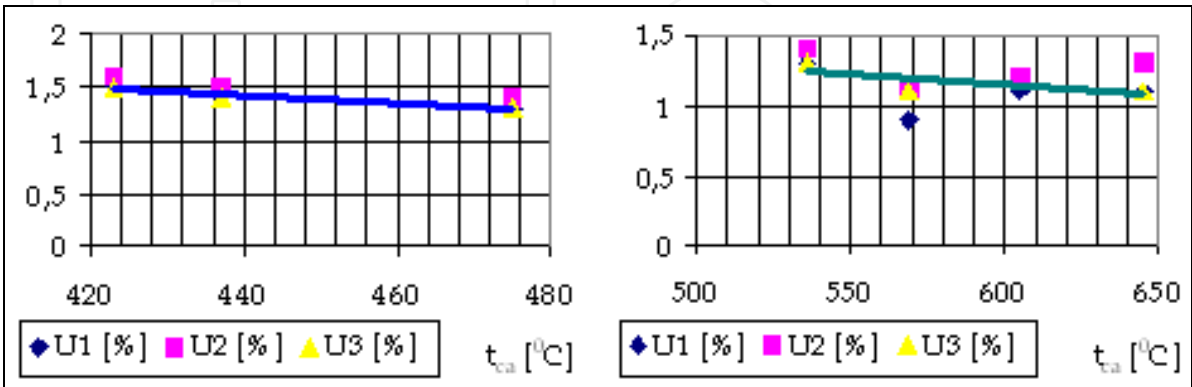


Fig. 19. Variation of distortion coefficients from the fundamental (THD) for voltage depending on the flue gases temperature at the outlet of the afterburning chamber for version gas turbine + heat recovery steam generator (left) and version gas turbine + afterburning + heat recovery steam generator (right)

The numerical simulations (fig. 20, right) indicate NO_x emissions three times lower for the ST 18-R module compared to the old ST 18 model at nominal working regime temperature of the afterburning at 2xST 18 Cogenerative Power Plant (770 °C).

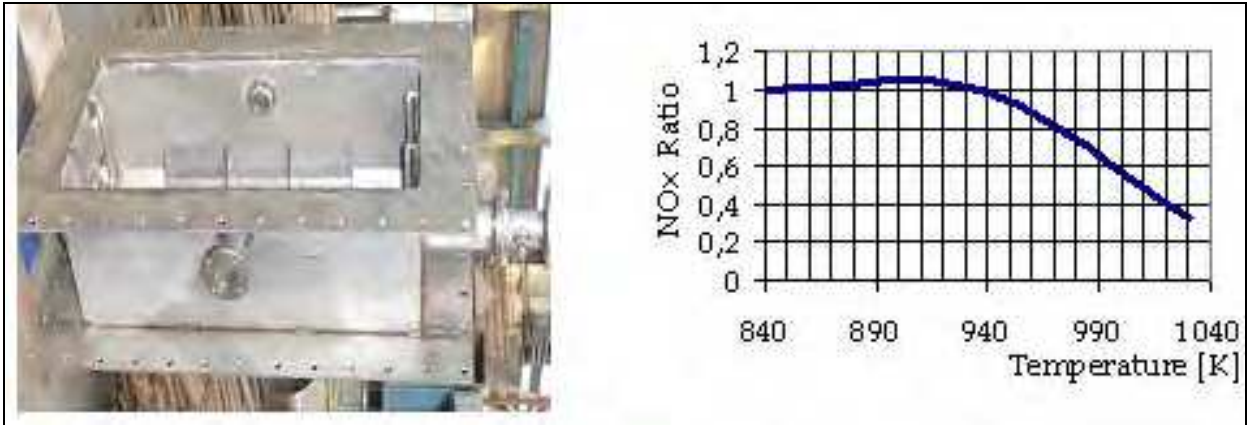


Fig. 20. Burner with three burning modules ST 18-R (left) and the variation of the NO_x ratio depending on the flue gases temperature for modules ST 18 and ST 18-R (right)

6.2.3 Experimental data obtained on test bench

For a thorough investigation of the processes and for eliminating some disturbing factors from the plant test bench examinations were required for the data obtained at 2xST 18 Plant as well as for the numerical results obtained in CFD environment. For this purpose there was designed and manufactured the gas fuel burner INCDT APC 1MGN – UPB (fig. 21, left) with a thermal power of approximately 350 kW, allowing the testing of only one ST 18 or ST 18-15 burning module and adaptable for other geometrical configurations in the same overall dimensions. The natural gas is introduced through a connector in the lower area and the air through a lateral flanged connector. The experiments for the ST 18 (or angled ST 18-15) module took place on the test bench of University Politehnica Bucharest (UPB), Department of Classic and Thermo-mechanical Nuclear Equipment (fig. 21, right). The tests have been made with natural gas and fresh air for different natural gas flow rates (0.5; 0.7 and 0.88 m³/h). The experimental cell was a rectangular enclosure (890x890x990 mm) with a truncated pyramid segment connected to the exhaust stack. The walls are made of glass allowing the observation of the flame, one side door providing access (fig. 21, centre and right).

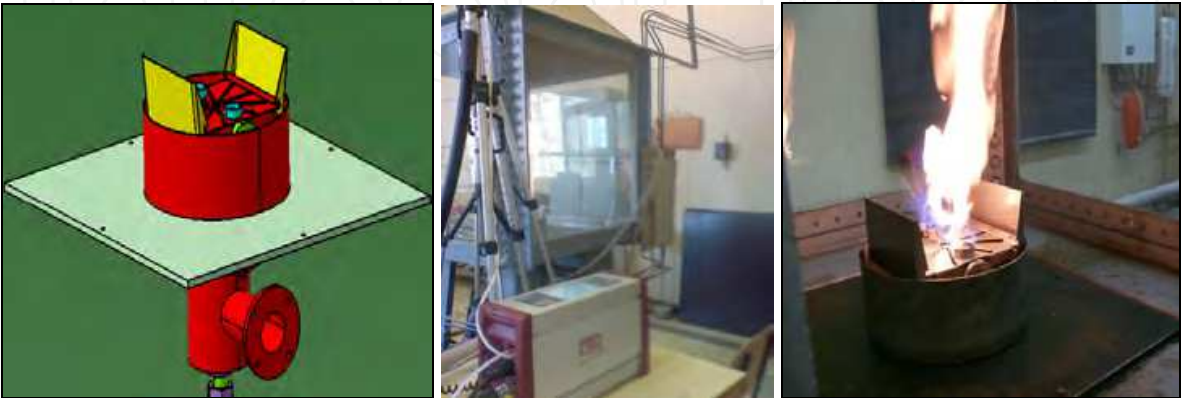


Fig. 21. Burner INCDT APC 1MGN – UPB with module ST 18-15, 3D design (left) and UPB test bench testing (centre and right)

The connection of the burner to the natural gas network was made through a hose and the one to the air fan through a removable flanged assembly. The placement of the burner was achieved through a plate fixed by screws. The emission measurements have been performed with a gas analyser MRU - Analyzer Vario Plus Ind. (fig. 21 centre) and the noise has been monitored with a sound level meter 01 dB Metravib SOLO mounted in the upper area of the enclosure. The outer superficial temperature profile has been determined with the help of a type Ti45FT Fluke infrared camera, the flame being sighted with the access door open (fig. 21, left). The measurements for emissions and noise at the three flow rates have been performed with the access door open. The temperature distribution in the flame has been determined with the help of three thermocouples (type PtRh30% - PtRh46%) placed on a holder on the height estimated for the flame development. The counting of the thermocouples starting from the base was: T_{FL1} , T_{FL2} and T_{FL3} . It was noticed a more homogenous distribution and a slower increase in temperature in the flame on ST 18-15 module, as seen in fig. 22. This also results from table 6 presenting parameters in the infrared recording - module ST 18 (left) and ST 18-15 (right). The areas occupied by the high temperature isotherms are significantly increased for module ST 18-15. Compared to module ST 18, the flame fills more the burning point, it shortens, the temperature distribution is more homogenous and the NO_x and CO emissions decrease. For the flow rate of natural gas of $0.88\text{ m}^3/\text{h}$ a decrease in the NO_x emissions occurs, over 30 % for module ST 18-15 compared to ST 18 (fig. 23). However the values of noise for the module ST 18-15 are higher than for ST 18 due to increased turbulence (fig. 24). This phenomenon may be better observed particularly for high flow rates ($0.88\text{ m}^3/\text{h}$). The researches conducted until present have shown the superiority of module ST 18-15, the numerical results being validated by the experimental ones obtained on the test bench.

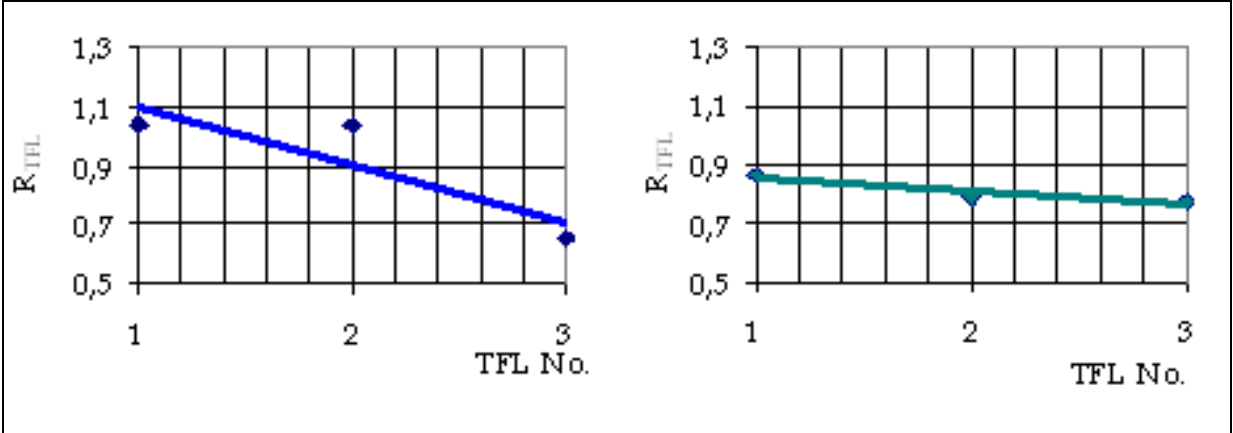


Fig. 22. Variation of the temperature ratios in the flame (for T_{FL1} , T_{FL2} and T_{FL3}), corresponding to modules ST 18-15 and ST 18 at $Q_{combs} = 0.5\text{ m}^3/\text{h}$ (left) and $Q_{combs} = 0.88\text{ m}^3/\text{h}$ (right)

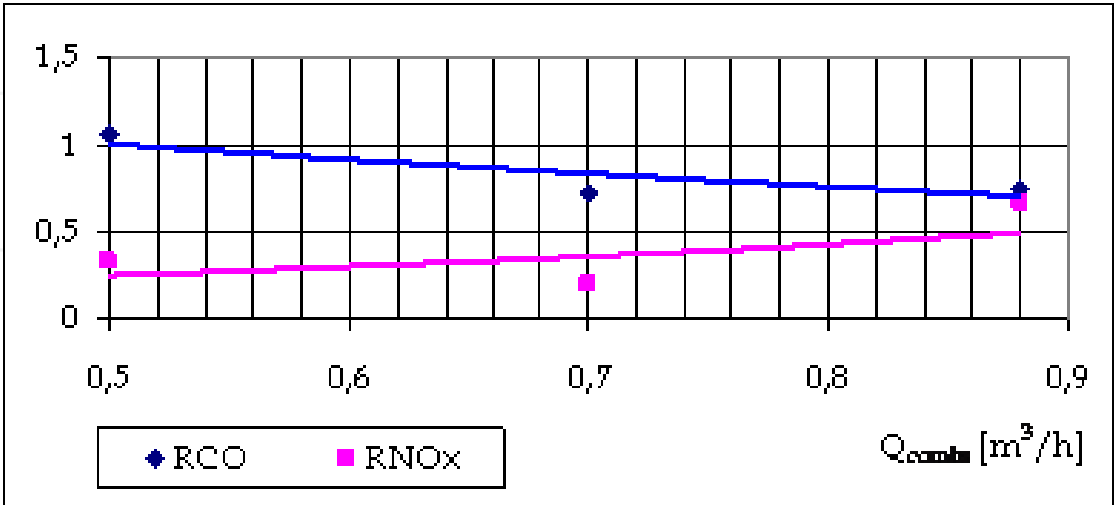


Fig. 23. The CO and NO_x ratios variation corresponding to ST 18-15 and ST 18 modules depending on natural gas volume flow

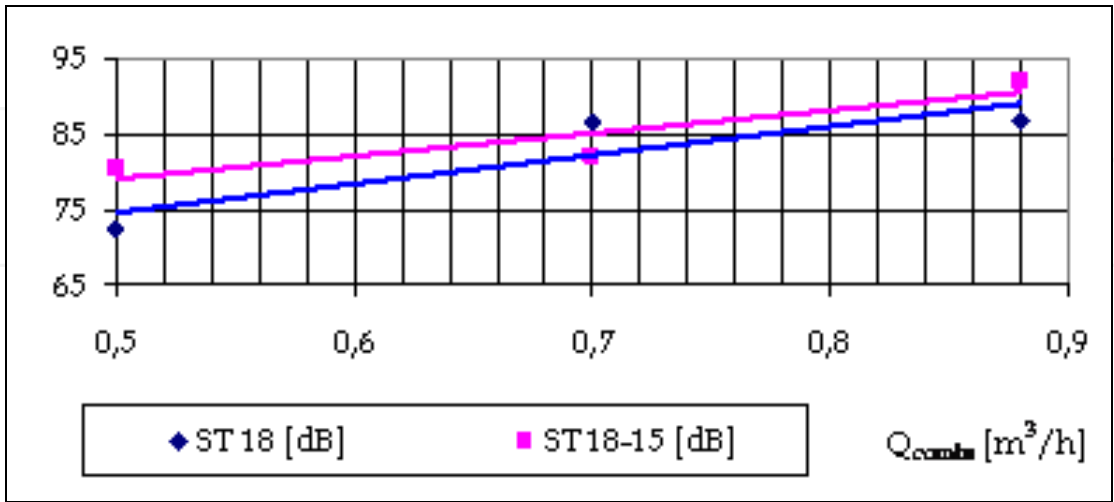


Fig. 24. Noise variation corresponding to ST 18-15 and ST 18 modules, depending on natural gas volume flow

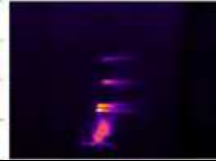
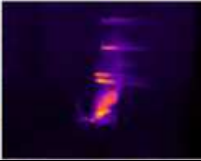
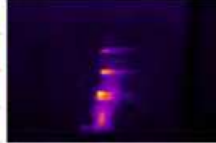
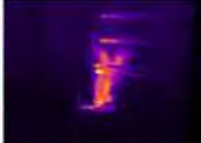
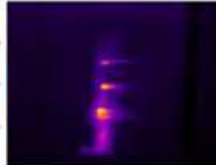
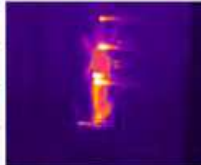
No.	Natural gas flow rate Q_{combs} [m ³ /h]	Isotherms (according to the burning module type)	
		Module ST 18	Module ST 18-15
1	0,5		
2	0,7		
3	0,88		

Table 6. Isotherms at the infrared recording for modules ST 18 (left) and ST 18-15 (right) depending on the natural gas flow rate

7. Conclusions

The new generation of afterburning installations will need to respond to the performance requirements of the „smart“ aggregates to automatically consider emissions, energetic efficiency and process requirements. The researches conducted at Suplacu de Barcau 2xST 18 Cogenerative Power Plant have analyzed the afterburning installation as integrated in the cogenerative group. Based on the measurements and the numerical results, the burning modules have been redesigned, experiments on the test bench have been conducted in order to establish the performances of the new generation of modular burners and the working regimes of the gas turbine have been established for water injection and afterburning cases. For the independent working of the TA-2 gas turbine, the numerical simulations had shown the possibility of 50% decrease in the NO_x emissions. However the modelling of the assembly TA-2 gas turbine with water injection and afterburning has shown that the NO_x emissions decrease (at the working regime defined by T_m = 1063 K) is possible only to 40 ppm (below 30 %). This confirms the necessity of a fine control of the quantity of water injected in the gas turbine particularly when a significant decrease in NO_x emissions is aimed. Future researches will involve test bench experimentations of the gas turbine working on natural gas with water injection, coupled with the multi-module afterburning installation. The experimental data should validate the elaborated numerical model and will constitute the design input data for a new afterburning installation.

8. Acknowledgments

The researches conducted at Suplacu de Barcau 2xST 18 Cogenerative Power Plant have been performed based on contracts 22-108/2008 and 21-056/2007 (Programme “Partnerships in priority fields”) financed by Romanian Ministry of Education, Research, Youth and Sports. The consortium involved in the projects includes several Romanian companies: National Research and Development Institute for Gas Turbines COMOTI -

Bucharest, SC OMV PETROM SA, UPB CCT - Bucharest, SC OVM ICCPET SA - Bucharest, SC ICEMENERG SA - Bucharest, SC ERG SRL - Cluj, SC TERMOCAD SRL - Cluj.

9. References

- Barbu, E., Rosu, I. & Turcu G. (2006). Supraincalzitorul cazanelor de la centrala cogenerativa 2xST 18 – Suplacu de Barcau, *ETCNEUR – 2006*, pp. 9-12, ISBN 973-7984-49-8, Bucuresti, 6-7 iulie 2006
- Barbu, E., Ionescu, S., Vilag, V., Vilcu, C., Popescu, J., Ionescu, A., Petcu, R., Prisecaru, T., Pop E. & Toma T. (2010). Integrated analysis of afterburning in a gas turbine cogenerative power plant on gaseous fuel, *WSEAS Transaction on Environment and Development*, Vol. 6,. Issue 6, June 2010, pp. 405-416, ISSN 1790-5079
- Barbu, E., Fetea, Gh., Petcu, R. & Vataman, I. (2010). *Arzator de postardere multimodular pe combustibil gazos*, Dosar OSIM nr. A/00999 din 21.10.2010
- Benini, E., Pandolfo, S. & Zoppellari, S. (2009). Reduction of NO emissions in a turbojet combustor by direct water/steam injection: numerical and experimental assessment, *Applied Thermal Engineering*, doi: 10.1016/j.applthermaleng.2009.06.004
- Carlanescu, C., Ursescu, D. & Manea, I. (1997). *Turbomotoare de aviatie – Aplicatii industriale*, Editura Didactica si Pedagogica, Bucuresti
- Carlanescu, C., Manea, I., Ion, C. & Sterie, St. (1998). *Turbomotoare – Fenomenologia producerii si controlul noxelor*, Editura Academiei Tehnice Militare, Bucuresti
- Conroy, J. (2003). Improving duct burner performance through maintenance and inspection, *Energy-Tech*, February 2003, <http://www.energy-tech.com/article.cfm?id=17543>
- Ganapathy, V. (2001). Superheaters: design and performance, *Hydrocarbon processing*, July 2001, <http://www.angelfire.com/md3/vganapathy/superhtr.pdf>
- McBride, B.J. & Gordon, S., (1992) *Computer Program for Calculating and Fitting Thermodynamic Functions*, NASA Lewis Research Center, NASA RP-1271, Cleveland, USA, <http://www.grc.nasa.gov/WWW/CEAWeb/RP-1271.pdf>
- Neaga, C. (2005). *Tratat de generatoare de abur*. vol. III, Editura Printech, Bucuresti, ISBN 973-718-262-6
- Petcu, R., (2010). *Contributii teoretice si experimentale la utilizarea gazului de depozit ca sursa de energie*, Teza de doctorat - Decizie Senat nr. 100/12.02.2010, Bucuresti
- Popescu, J., Vilag V., Barbu, E., Silivestru, V. & Stanciu, V. (2009). Estimation and reduction of pollutant level on methane combustion in gas turbines, *Proceedings of the „3rd WSEAS International Conference on Waste Management, Water Pollution, Air Pollution, Indoor Climate – WWAI’09”*, pp. 447-451, ISBN 978-960-474-093-2, University of La Laguna, Tenerife, Canary Islands, Spain, July 1-3, 2009
- Public Interest Energy Research, [PIER]. (2002). *Active control for reducing the formation of nitrogen oxides in industrial gas burners and stationary gas turbines*, California Energy Commission, http://www.energy.ca.gov/reports/2002-01-10_600-00-009.PDF
- Zehe, M.J., Gordon, S. & McBride, B.J. (2002), *CAP: A Computer Code for Generating Tabular Thermodynamic Functions from NASA Lewis Coefficients*, NASA Glenn Research Center, NASA TP–2001-210959-REV1, Cleveland, Ohio, USA, <http://www.grc.nasa.gov/WWW/CEAWeb/TP-2001-210959-REV1.pdf>



Advances in Gas Turbine Technology

Edited by Dr. Ernesto Benini

ISBN 978-953-307-611-9

Hard cover, 526 pages

Publisher InTech

Published online 04, November, 2011

Published in print edition November, 2011

Gas turbine engines will still represent a key technology in the next 20-year energy scenarios, either in stand-alone applications or in combination with other power generation equipment. This book intends in fact to provide an updated picture as well as a perspective vision of some of the major improvements that characterize the gas turbine technology in different applications, from marine and aircraft propulsion to industrial and stationary power generation. Therefore, the target audience for it involves design, analyst, materials and maintenance engineers. Also manufacturers, researchers and scientists will benefit from the timely and accurate information provided in this volume. The book is organized into five main sections including 21 chapters overall: (I) Aero and Marine Gas Turbines, (II) Gas Turbine Systems, (III) Heat Transfer, (IV) Combustion and (V) Materials and Fabrication.

How to reference

In order to correctly reference this scholarly work, feel free to copy and paste the following:

Ene Barbu, Valeriu Vilag, Jeni Popescu, Silviu Ionescu, Adina Ionescu, Romulus Petcu, Cleopatra Cuciumita, Mihaiella Cretu, Constantin Vilcu and Tudor Prisecaru (2011). Afterburning Installation Integration into a Cogeneration Power Plant with Gas Turbine by Numerical and Experimental Analysis, *Advances in Gas Turbine Technology*, Dr. Ernesto Benini (Ed.), ISBN: 978-953-307-611-9, InTech, Available from: <http://www.intechopen.com/books/advances-in-gas-turbine-technology/afterburning-installation-integration-into-a-cogeneration-power-plant-with-gas-turbine-by-numerical->

INTECH
open science | open minds

InTech Europe

University Campus STeP Ri
Slavka Krautzeka 83/A
51000 Rijeka, Croatia
Phone: +385 (51) 770 447
Fax: +385 (51) 686 166
www.intechopen.com

InTech China

Unit 405, Office Block, Hotel Equatorial Shanghai
No.65, Yan An Road (West), Shanghai, 200040, China
中国上海市延安西路65号上海国际贵都大饭店办公楼405单元
Phone: +86-21-62489820
Fax: +86-21-62489821

© 2011 The Author(s). Licensee IntechOpen. This is an open access article distributed under the terms of the [Creative Commons Attribution 3.0 License](https://creativecommons.org/licenses/by/3.0/), which permits unrestricted use, distribution, and reproduction in any medium, provided the original work is properly cited.

IntechOpen

IntechOpen